International Journal of Engineering Research-Online
A Peer Reviewed International Journal
Articles available online http://www.ijoer.in; editorijoer@gmail.com

Vol.5., Issue.3, 2017
May-June

RESEARCH ARTICLE

ISSN: 2321-7758

ADSORPTION DYNAMICS AND KINETIC STUDIES OF As (III) ION ONTO MAGNETIC 'Al-Ni' NANOFERRITES (ANF)

GURRALA ALLURAIAH[1], KONGARA SHOBHA RANI[2]

[1]Lecturer in Chemistry, S.V Arts and Science College, Giddalur, Prakasam District
[2]Lecturer in Chemistry, VSR & NVR College, Tenali, Guntur District

GURRALA ALLURAIAH

Article Received :10-5-2017
Article Accepted :16-6-2017
Available online: 30-6-2017

ABSTRACT

This paper presents the studies regarding the synthesis, characterization and application of Al-Ni nanoferrite nanoparticles in the adsorption of As (III) from aqueous media. The obtained cobalt ferrite was investigated by FTIR spectroscopy, X-ray diffraction, SEM coupled with EDX, investigations which showed that the obtained particles are homogeneous as shape and size. Due to the obtained nanoparticles and due to the affinity of arsenic toward iron, the obtained cobalt ferrite was applied with success as adsorbent in the removal process of arsenic from aqueous solutions. The optimal parameters affecting the adsorption of arsenic ions As(III) on magnetic aluminium-nickel nanoferrites (ANF) as adsorbent sample were determined by conducting batch experiments. The adsorption of As(III) was strongly dependent on pH, agitation time and initial adsorbate concentration. The maximum adsorption capacity for arsenic (III) obtained from Langmuir model was found to be 67.10 mg/g and the kinetics data followed pseudo-first order better than pseudo-second order. Energy dispersive SEM-EDX study proved the removal of arsenic from aqueous media

Keywords: Al-Ni nanoferrite, X-ray diffraction, adsorption, arsenic removal, Langmuir isotherm.

1.0 Introduction

Contamination of environment with a wide array of organic and inorganic pollutants is a serious health concern. Heavy metals are major inorganic pollutant owing to their high toxicity and non biodegradability[1]. They accumulate in living tissues through food chain and cause various diseases and disorders[2]. Their removal from natural resources is considered as primarily important in the modern era. Arsenic, a metalloid, is notoriously harmful to human health but although other species such as bacteria use arsenic as a respiratory metabolite. Arsenic occurs in two major forms - inorganic and the organic. The inorganic arsenic is more toxic than the organic form and is predominantly seen in drinking water, whereas organic form is seen in sea foods[3]. Inorganic arsenic are the components of geological formation and extracted into ground water, the contamination can also be due to mining, human activities and natural well waters with high concentrations of arsenic. These contaminations extort into drinking water and make it more toxic than organic arsenic. The inorganic forms of arsenic are arsenate, As (V) and arsenite As (III). Arsenite is the reduced inorganic species and is more toxic than the oxidized form arsenate[4]. The common method of As (III) ions removal from aqueous system is chemical precipitation, ion exchange, membrane processes, electrodialysis and adsorption. Ion exchange, reverse osmosis and electrodialysis are efficient for As (III) removal but the cost is relatively high. Methods such as co-precipitation, membrane techniques and solvent extraction are challenged by the removal of lower concentrations of metals from solution[5]. Precipitation produces large quantities of heavy metals rich waste sludge; ion exchange and

biomass methods are costly and cannot be readily applied to large scale applications. The process of adsorption has received considerable attention as one of the most suitable method for the removal of heavy metals from aqueous solutions. This process is suitable even when the metal ions are present in concentration as low as 1 mg/L[6].

Role of nanomaterials for the remediation of waste-water is a thrust area of research. Nanomaterials play a pivotal role in physical, chemical and biomedical fields due to their high surface energies. Their role as adsorbents is a thrust area of research. Ferrites are the mixed metal oxides with ferric oxide (Fe_2O_3) as their main component. AB_2O_4 is the general formula for spinel ferrites, where tetrahedral-A sites and octahedral-B sites are occupied by metal cations. Stable and non-toxic nature of nano phase spinel ferrites along with their insolubility in water and high surface area can make them potential adsorbents for removing contaminants from water[7]. The properties of ferrite nanoparticles (NPs) are influenced by the composition and microstructure which is sensitive to the preparation methodology[8]. Nickel substituted aluminum nano-ferrites were promising material for the microwave device applications since these were less sensitive to the stress and have higher Curie temperature (Tc). Ni-Al ferrites are low cost materials and have important magnetic and adsorption properties for technological/ environmental applications[9]. Recently, the diamagnetic substitution in mixed ferrites has received special attention. The role played by the substituent in modifying the physical properties of basic ferrites and the mechanism behind enhanced magnetic response is not widely studied. In the present study Aluminium-Nickel magnetic ferrite nanoparticles (ANF) were synthesized by sol-gel method. Synthesized ferrite ANF was characterized by X-ray diffraction (XRD), SEM-EDX, FT-IR spectroscopy.

2.0 Experimental

2.1 Materials

All the reagents are of analytical grade and are used as-received without further purification. Nickel nitrate $Ni(NO_3)_2{\cdot}6H_2O$, $(Al(NO_3)_3{\cdot}9H_2O)$, and Ferric nitrate $[Fe(NO_3)_3{\cdot}9H_2O]$ obtained from Merck-India are taken as oxidants. All reagents were prepared using double distilled water. Stock solution of arsenite was prepared using analytical grade sodium arsenite ($NaAsO_2$, Merck, India). Working arsenic solutions of different concentrations were prepared by diluting stock arsenic solutions.

2.2 Synthesis of Nickel-Aluminum Nanoferrites

ANF ($Ni_{0.4}$ $Al_{0.2}Fe_2O_4$) nanoferrites were prepared by sol-gel auto-ignition method. The A.R grade Citric acid ($C_6H_8O_7$), Nickel nitrate Aluminum nitrate, Ferric nitrate was used as starting materials. The molar ratio of metal nitrates to citric acid was takes as 1:1. The metal nitrates were dissolved together in a minimum amount of de-ionized water to get clear solution. An aqueous solution of citric acid was mixed with metal nitrates solutions, and then ammonia solution was slowly added to adjust the pH at 7. The mixed solution was moved on to a hot plate with continuous stirring at 80˚C. During evaporation, the solution became viscous and finally formed a very viscous brown gel. When finally all remaining water was released from the mixture, the sticky mass began to bubble. After several minutes the gel automatically ignited and burnt with glowing flints. The decomposition reaction would not stop before the whole citrate complex was consumed. The auto-ignition was completed within a minute, yielding the brown colored ashes termed as a precursor. The as-prepared powders of all the samples were heated at 600˚C for 2 hours in air to get the final products. The burnt powder was ground in Agate Mortar and Pestle to get a fine ferrite powder, finally used as Adsorbent for the removal of Arsenic ion

2.3 Characterization of ANF sample

Phase structure of all the prepared sample was characterized by X-ray diffraction (XRD) with Cu-Kα radiation and graphically presented in Figure 1. Surface morphology and elemental analysis of ANF sample was confirmed by SEM-EDX technique. The shape and size of the grain samples was determined from the micro graphs taken using the scanning electron microscope (SEM) (JEOL JSM-5600LV) equipped with EDX analyzer. The presence of characteristic peaks of ANF spinel ANF nanocomposite is investigated into a 400-4000 cm-1 range by spectrophotometer, Nicolet iS10 FT-IR spectrometer. The analyses were run using the KBr pellet technique.

2.4 Arsenic Analysis

Arsenic analysis was carried out using a Varian Spectra AA 880 graphite furnace atomic absorption spectrometer (AAS, Avanta Sigma, GBC Scientific Equipment Ltd.), with Zeeman background correction. All measurements were based on integrated absorbance and performed at 193.7 nm by using a hollow cathode lamp. Pretreatment temperature of the furnace was 1400 K and atomization temperature was 2500 K. The calibration range was 20 to 100 µg/L of arsenic.

2.5 Adsorbent Characterization

The phase formation of ferrite materials was investigated by X-ray diffraction (XRD). The XRD analysis on the prepared samples was made using a SCINTAG X'TRA AA85516 (Thermo ARL) X-ray diffractometer equipped with a Peltier cooled Si solid detector. The chemical vibrational mode of ferrite samples was studied by Fourier transform infrared spectroscopy (FTIR). The sample discs were prepared by mixing of 1 mg of powdered carbon with 500 mg of KBr (Merck-spectroscopy quality) in an agate mortar, then pressing the resulting mixture successively under a pressure of 5 tones/ cm^2 for about 5 min., and at 10 tones/ cm^2 for 5 min., under vacuum. The spectra were measured from 4000 to 400 cm^{-1} on a JASCO-FTIR-5300 model. The morphology analysis of the samples was carried out by scanning electron microscopy (SEM). The microphotographs of these samples were recorded using SEM JEOL model, JSM-5600 equipped with EDX Analyzer, an accelerating voltage of 5 kV, at high vacuum mode. The maximum magnification possible in the equipment is 3,00,000 times with a resolution of 3 nm, typically setting at various magnifications for all the samples of study. The saturation magnetization measurements of all the samples were carried out at room temperature using Pulse Field Magnetic Hysteresis Loop Tracer. Magnetization, coercivity and remanence magnetization were calculated from the hysteresis loops

2.6 Batch Adsorption Studies

A comparative study for the effectiveness of ANF adsorbent sample for the As(III) removal was conducted. Batch experiments were carried out in a temperature controlled mechanical shaker (Remi Shaker, India). Solution pH is an important factor for all water and wastewater treatment processes as it affects the speciation of the metals. Studies were conducted at different initial pH levels (2-10) to determine the effect on As(III) adsorption, Concentration rnage 5 to 10mg/L and Time 10-60 minutes. These samples were agitated in a mechanical shaker at 200 rpm at room temperature 30°C until equilibrium was reached. Samples were filtered through Whatman no.42 filter paper and the residual As(III) concentration was determined using AAS.

The removal efficiency was calculated with equation (1), where C_i is the initial As (III) ion concentration in the solution prior to the contact test, and C_f is the As (III) ion concentration determined from the AAS characterization:

$$\% \, Removal = \frac{(Ci - Cf)}{Ci} \times 100 \quad \ldots(1)$$

3.0 Results and discussion

3.1 XRD Studies

X-ray powder diffractometer (XRD) with Cu Kα (λ=1.541 78 Å) radiation was used to investigate the structure and phase formation of the prepared Al-Ni nanoferrtie sample. Figure 1 illustrates the XRD patterns obtained at room temperature. ANF sample showed well resolved diffraction peaks located at 2θ of 29.94°, 34.68 °, 36.5 °, 43.67 °, 53.7 °, 57.49 °, 64.02 ° and corresponding planes (220), (311), (222), (400), (422), (511) and (440) are indexed with the lattice parameter of a = 8.339 Å which confirms the formation of FCC spinel phase in accordance with card number JCPDS 49.6172. The characteristic peaks of the ANF can be well indexed as cubic spinel phase. Moreover, the intense and sharp peaks show that the ANF is well crystallized. The Scherer formula is used to calculate crystallite size of Al-$NiFe_2O_4$ nanoparticles 20±1 nm, Scherer formula is given in Eq. (2):

$$D = \frac{0.9\lambda}{\beta cos\theta} \text{-------(2)}$$

Whereas 0.9 is crystal shape factor, λ (Å) is the wavelength of incident X-rays, is Full Width Half Maximum (FWHM) and 2θ is the diffraction angle.

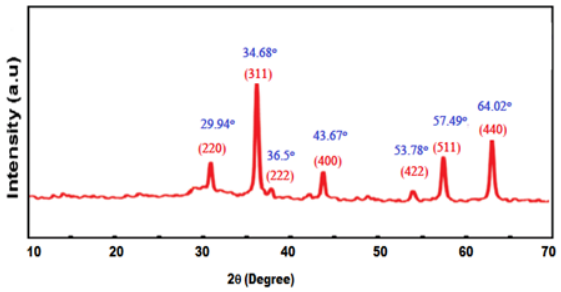

Figure 1: XRD patterns of ANF

3.2 FT-IR Study

Infra red (IR) absorption spectroscopy helps to identify the spinel structure. The three typical vibrational bands associated with spinel structure[10] are at (1) 600-550cm^{-1} (2) 450-385 cm^{-1} (3) 350-330cm^{-1} for metal-oxygen band. Fourier transformed infra red (FTIR) spectroscopy studies of the nano particle ferrite samples were carried out between 1000 - 400 cm^{-1} as shown in figure 2. Out of the two bands the high frequency (υ_1) band is attributed to the tetrahedral metal-oxygen bond and second frequency (υ_2) band to the octahedral metal-oxygen bond.IR spectral data of all the ferrite samples prepared by these methods are found to show two peaks in the range 578-564 cm -1 and 472- 443 cm-1 which are in agreement with the reported value[11].

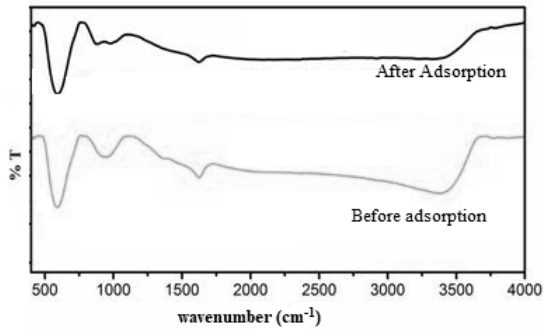

Figure 2: FTIR Spectra of ANF before and after adsorption

A broad and strong band stretch was observed from 3000 to 3500 cm^{-1}, indicating the presence of free or hydrogen bonded –OH groups present on the adsorbent surface[12] (alcohols and carboxylic acids). The peak present at 3451.9 cm^{-1} before adsorption broaden and shifted towards 3464.9 cm^{-1} after adsorption may be due to replacement of -OH bonded -H ion with As(III) ion.

3.3 SEM-EDX Study

Particle size and morphology were observed using SEM as shown in Figure 3 It is clear from the figure that samples consisted of fine particles. The surface morphology of the three types of nanoparticles shows some variation. The particles were mostly spheroid and loosed. Macropores are also clearly visible in the SEM images.

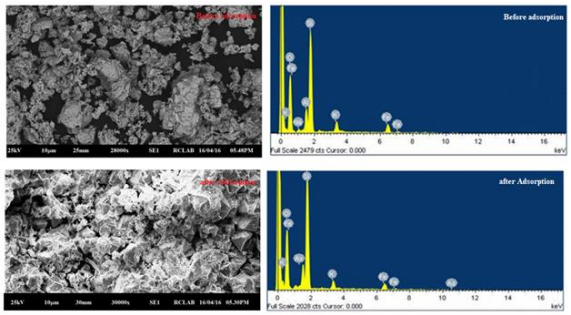

Figure 3: SEM EDX Spectra of ANF before and after adsorption of As^{3+}.

Figure 3 shows SEM of exhausted adsorbent clearly indicates the presence of new shiny bulky particles and layer over the surface of metal loaded adsorbent those are absent from the native adsorbent before metal loading, and thus observed significant visible changes in the morphology of ANF before and after As(III) sorption. Figure 3 shows the SEM-EDX image of ANF sample before and after adsorption. This image is representative of the porous structure of ANF. The main elements of ANF before adsorption comprise carbon, oxygen, Fe, Ni, Al and Oxygen, Carbon. After adsorption, As^{3+} reacts with nanosurface to form surface precipitation. The result corresponds to the expected assumption from the XRD pattern. Moreover, the adsorption mechanism can be demonstrated.

3.4 Effect of dose and Contact time on the removal of As(III) removal by ANF

The effects of dosage and contact time for ANF on the removal of As(III) ion from their aqueous solutions are shown in Figure 4. The effect of contact time on the adsorption of metal was investigated. Figure 4 shows the percent metal ion removal with respect to time. Contact time is one of the most effective factors in batch adsorption process. Adsorption rate initially increased rapidly, and the optimal removal efficiency was reached within about 60 min. Further increase in contact time did not show significant change in equilibrium concentration; that is, the adsorption phase reached equilibrium. From this figure it can be seen that there was a remarkable increase in the removal of

metal ion with increasing dosage of the used adsorbent (ANF). This probably arises from the increase in the adsorption capacity with increase of the concentration of ANF in the mixture. The shaking time was one hour at 25°C for all experiments that were performed in this work in order to achieve a full equilibration for all doses of the ANF that were synthesized[13]. In terms of the effect of contact time on dye removal also there was a progressive increase in the percentage of dye removal with duration time. This can be attributed to increase uptake capacity of the adsorbent with increase of time and does not reach the maximum adsorption capacity in the range of one hour of adsorption process. These results are shown in Figure 4.

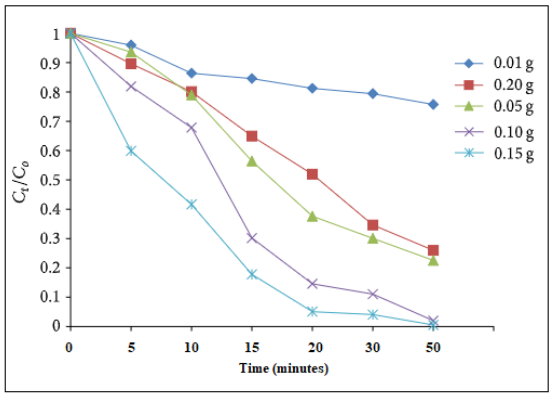

Figure 4: The effect of dosage and contact time of ANF on the removal of As^{3+} ion

3.5 Adsorption Isotherm Study

Study of adsorption isotherms was investigated using both Langmuir and Freundlich isotherms for adsorption of As(III) ion on the ANF sample that was synthesized from spinel ferrites. Langmuir adsorption isotherm is based on the formation of homogeneous monolayer on surface of the adsorbent[14]. For this type of homogeneous adsorption, all adsorption sites are considered to be energetically equivalent. For the physical adsorption, Freundlich equation is applied to follow adsorption isotherm. Both Langmuir and Freundlich isotherms can be explained mathematically as summarized in the following relations:

Freundlich isotherm : $\log qe = \log K_f + (1/n) \log Ce$

Langmuir isotherm : $(Ce/qe) = (1/ab) + (Ce/a)$

Where, K_f and 1/n are the measures of adsorption capacity and intensity of adsorption respectively, qe is the amount of As(III) ion adsorbed per unit weight of the adsorbent ANF (in mg/g), Ce is the equilibrium concentration of As(III) ion (mg/L); a and b are Langmuir constants. The values of K_f and 1/n have been obtained from the linear correlations of log Qe against log Ce (Figure 5) and the Langmuir constants have been also determined from the linear correlations of 1/Qe against 1/Ce (Figure 6). As mentioned above, maximum adsorption capacity for the ANF sample can be obtained using Langmuir equation. In this context, reaction conditions that were applied in this part were as follows: temperature was 25°C, pH 5.5, and the initial concentration of As(III) ion was 40 mg/L The amount of the used ANF sample ranged from 0.05 to 0.20 g with increasing rate of 0.05 g for each dose. The obtained results for the isotherms constants are summarized in Table 1. These results are represented graphically in Figures 5 and 6 as against. These results were more fitted with Freundlich isotherm. This arises from a high value of correlation coefficient for these results.

Table 1: Langmuir and Freundlich isotherm constants

Isotherms	Constants/correlation coefficients	Values
Langmuir	R^2	0.9698
	q_e	67.10
	K_L	0.506
Freundlich	R^2	0.6535
	K_f	22.36
	n	2.427

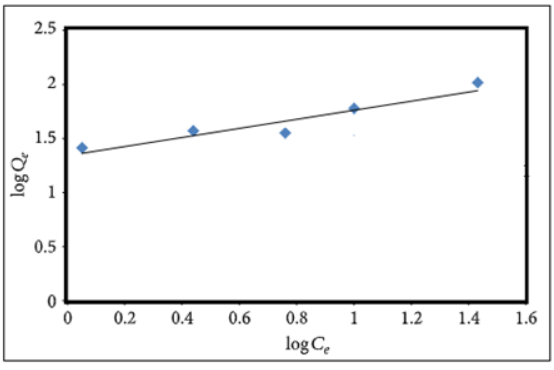

Figure 5: The linear Freundlich adsorption isotherms for As(III) ion adsorption by the ANF

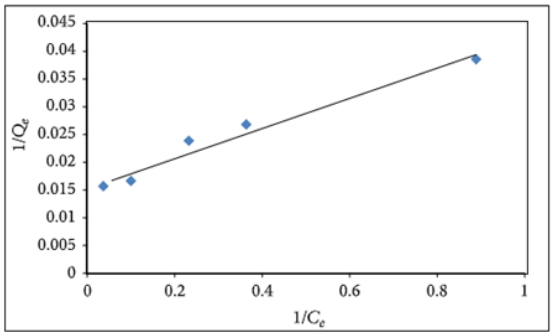

Figure 6: The linear Langmuir adsorption isotherms for As(III) ion adsorption by the ANF.

3.6 Kinetics Study

Several models are available to express the mechanism of adsorption of solute onto the sorbent. To investigate the mechanism of adsorption of As^{3+}, both Pseudo first order (Lagergren) and pseudo-second-order equation were used.

The linear (integrated under the boundary conditions)form of pseudo first-order model is depicted as follows:

$\ln(qe - qt) = \ln qe - k_1\, t$---(3)

where k_1 is the pseudofirst-order rate constant, qe and qt are the adsorption capacity of the adsorbent at equilibrium and at time t, respectively.

The logarithmic term ln (qe-qt) indicates that qe is given a maximum measured value. From the data plotted in Figure 7, the maximum value is shown by the second last data point measured at 30 min. So for ANF qe =0.3647 mg/g and the data in Figure 7, plotted according to (eq 3), is shown in Figure 7. It is clear from the value of R^2 that the linear fit is satisfactory.

The pseudosecond-order model can be expressed as follows:

$\frac{t}{qt} = \frac{1}{k_2 q_e^2} + \frac{t}{qe}$---(4)

where $k_2$is the pseudosecond-order rate constant.

Thus plotting t/qt versus 't' will give a straight line, as shown in Figure 8. The value of , , and can be determined from the slope and intercept of the plot. From the figure 8, the R2 value (0.998) is more than the previous model (0.7624). Therefore, the amount of As (III) uptake at equilibrium calculated using the pseudo-second-order equation was consistent with that obtained from the experiment. The kinetic data fitted closely with the pseudo-second order reaction, indicating that As^{3+} adsorption onto ANF is chemisorptions.

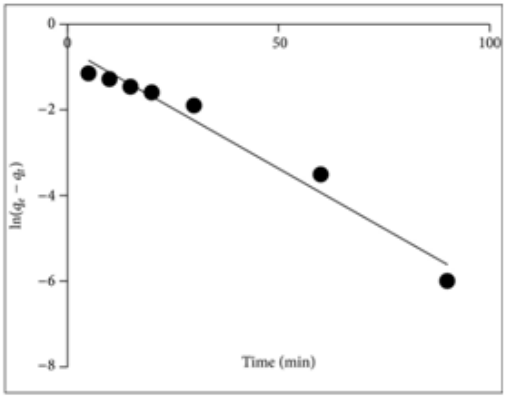

Figure 7: Pseudo First-order kinetic plot for the adsorption of As(III) ion,

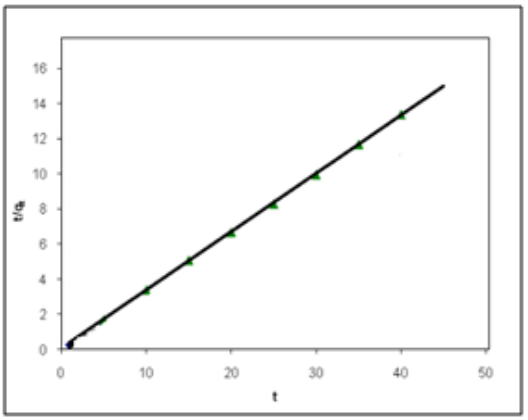

Figure 8: Pseudo second-order kinetic plot for the adsorption of As(III) ion,

3.7 Effect of pH

The effect of pH on removal of arsenic is shown in Figure 9. The study was done in the pH range of 3 to 12. It was found that the adsorption of arsenic ion gradually increases as the initial pH of the solution is raised from 3 to 7. The maximum removal of arsenic was found to be 71.3%, at pH 7. Hence, pH of the arsenic solution was maintained at 7 for further study. This agrees with the other results obtained on iron oxide coated on cement[15], carbon based adsorbents[16], and zero valent iron[17]. At pH more than 7, the removal process is very low. This is due to high OH– ion concentration, which reverses the process of removal, and hence the process of conversion of adsorbent into its OH– form plays an important role leaving behind arsenic in the aqueous solution. This is due to the effect of precipitation of Arsenic.

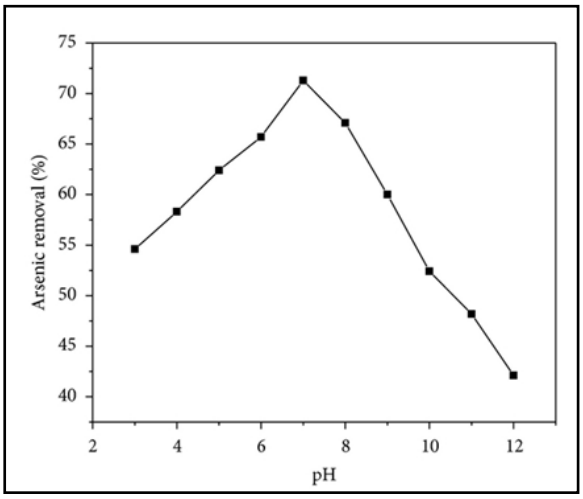

Figure 9: Effect of pH on adsorption of arsenic.

3.8 Magnetic properties

The magnetic parameters of prepared nanoferrite samples were calculated by using a vibrating sample magnetometer (VSM) in the range 5000 Oe, where the samples displayed the magnetic behaviour. The hysteresis loops (figure 10) were plotted from the VSM measurements, from which the saturation magnetisation values for the adsorbent sample ANF was calculated and represented graphically in Figure 10. It was evident from the hysteresis loops that the sample does not saturate completely. From the result it is clear that the saturation magnetization decreases with the substitution of Aluminium. This decrease can be explained based on the site occupancy of the cations and also the modification in the exchange effects caused by substituting Aluminium .The Fe^{3+} ions occupying the 'B' sites in the inverse spinal lattice are the main contributors of the magnetic properties. Al^{3+} has no unpaired electrons and is paramagnetic in nature. There is a significant decrease in the coercively with the substitution of Al^{3+}. This theory states that the factors such as microstrain, magneto crystalline anisotropy, magnetic particle morphology, magnetic domain size and size distribution in fluence the coercivity[11].

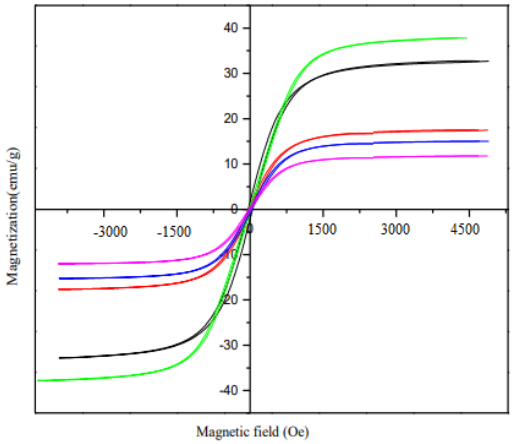

Figure 10: Magnetic hysteresis loop of ferroelectric content in the composite of ANF.

4.0 Conclusion

The sample nanoferrite Aluminium Nickel ferrite prepared by Sol-Gel method, followed by combustion- self decomposition was found to have spinel structure. This was confirmed using XRD and IR spectroscopy. The particle sizes were estimated using Scherer formula and were found to be in nano range, confirmed by SEM. Nano-materials produced by this method show high values of saturation magnetization. ANF material was employed for the removal of arsenic from the aqueous media at laboratory scale. The values of correlation coefficient of Langmuir isotherm is much higher than the other materials used for the removal of arsenic from aqueous media. The results showed that the 95 % of the arsenic has been removed from the water which is much higher than that of other adsorbents[18]. The high adsorption capacity and the % age removal of arsenic from water by Aluminium nickel ferrite suggest that this material have variety of potential applications and can be successfully used for the removal of arsenic.

References

1 Sharma Y C, Srivastava V K, Singh V K, Kaul S N and Weng C H (2009) Nano Adsorbents for the removal of metallic pollutants from water and waste water. *Environ Tech* **30**:583- 609

2 Umar F, Misbahul A K, Makshoof A and Janusz A K (2011) Effect of modification of environmentally friendly biosorbent wheat (*Triticum aestivum*) on the biosorptive

removal of cadmium(II) ions from aqueous solution. *Chem Eng J* **171**:400-10.

3 Taylor, J; Robinson, A; Johnson,N; Marroquin-Cardona, A; Brattin, B; Taylor, R; Phillips, T; "In Vitro Evaluation of Ferrihydrite as an Enterosorbent for Arsenic from Contaminated Drinking Water."Environmental Science and Technology, 2009, 43(14), 5501-5506.

4 Yan, H; Wang, N; Weinfeld, M; Cullen, W; Le, X; "Identification of Arsenic-Binding Proteins in Human Cells by Affinity Chromatography and Mass Spectrometry." Analytical Chemistry, 2009, 81(10), 4144-4152.

5 Valix M, Cheung W H and Zhang K (2006) Role of heteroatoms in activated carbon for removal of hexavalent chromium from wastewaters. *J Hazard Mater* **135**:395-405

6 Chong K H and Volesky B (1995) Description of two-metal biosorption equilibria by Langmuirtype models. *Biotech Bio Eng* **47**:451-60.

7 Khaleel A, Kapoor P N and Klabunde K J (1999) Nanocrystalline metal oxides as new adsorbent for air purification. *Nanostruct Mater* **11**:459-68.

8 Jacob B P, Kumar A, Pant R P, Singh S and Mohammed E M (2011) Influence of preparation method on structural and magnetic properties of nickel ferrite nanoparticles. *Bull Mat Sci* **34**:1345-50.

9 Mathew George, Swapnw S.Nair, Asha Mary John, P.A.Joy, M.R. Anantharaman, "Structural, magnetic and electrical properties of sol-gel prepared Li0.5Fe2.5O4 fine particles, J.Phys.D:Appl.Phys.39 (2006) 900-910.DOI:10.1088/0022-3727/39/5/002

10 R. D. Waldron. Phys. Rev., 1955, 99, 1727

11 Thanit Tangcharoen,, Anucha Ruangphanit, Wisanu Pecharapaa, Ceramics International 39 (2013) S239–S243

12 E. Pehlivan, T. Altun, S. Cetin, M. Iqbal Bhanger, Lead sorption by waste biomass of hazelnut and almond shell, Journal of hazardous materials, 167 (2009) 1203-1208.

13 R. Katal, M. S. Baei, H. T. Rahmati, and H. Esfandian, "Kinetic, isotherm and thermodynamic study of nitrate adsorption from aqueous solution using modified rice husk," Journal of Industrial and Engineering Chemistry, vol. 18, no. 1, pp. 295–302, 2012.

14 R. Sivaraj, R. Venckatesh, G. Gowri, and G. Sangeetha, "Activated carbon from eichornia crassipes as an adsorbent for the removal of dyes from aqueous solution," International Journal of Engineering Science and Innovative Technology, vol. 2, no. 6, pp. 2418–2427, 2010

15 S. Kundu and A. K. Gupta, "Arsenic adsorption onto iron oxide-coated cement (IOCC): regression analysis of equilibrium data with several isotherm models and their optimization," Chemical Engineering Journal, vol. 122, no. 1-2, pp. 93–106, 2006

16 J. Pattanayak, K. Mondal, S. Mathew, and S. B. Lalvani, "Parametric evaluation of the removal of As(V) and As(III) by carbon-based adsorbents," Carbon, vol. 38, no. 4, pp. 589–596, 2000.

17 C. Su and R. W. Puls, "Arsenate and arsenite removal by zerovalent iron: kinetics, redox transformation, and implications for in situ groundwater remediation," Environmental Science and Technology, vol. 35, no. 7, pp. 1487–1492, 2001.

18 Idrees M, Batool S (2017) Enhanced Aqueous Arsenic Absorbing Substituted Spinel Nickel Ferrite (NiFe2O4) Nano-Particles. Adv Recycling Waste Manag 2: 123. doi:10.4172/2475-7675.1000123